IEEE Access
Multidisciplinary ⋮ Rapid Review ⋮ Open Access Journal

Received January 30, 2021, accepted February 15, 2021, date of publication February 18, 2021, date of current version March 1, 2021.

Digital Object Identifier 10.1109/ACCESS.2021.3060115

A Backstepping Global Fast Terminal Sliding Mode Control for Trajectory Tracking Control of Industrial Robotic Manipulators

THANH NGUYEN TRUONG, ANH TUAN VO, AND HEE-JUN KANG
Department of Electrical, Electronic and Computer Engineering, University of Ulsan, Ulsan 44610, South Korea

Corresponding author: Hee-Jun Kang (hjkang@ulsan.ac.kr)

This research was supported by Basic Science Research Program through the National Research Foundation of Korea (NRF) funded by the Ministry of Education (NRF-2019R1D1A3A03103528).

ABSTRACT We propose a backstepping global fast terminal sliding mode control for trajectory tracking control of industrial robotic manipulators in this article. An integral of the global fast terminal sliding mode surface is firstly suggested to improve the dynamic performance and fast convergence of Sliding Mode Control (SMC) and Terminal SMC (TSMC), which also obtains a finite-time convergence. A controller is then developed from the proposed sliding surface using the backstepping control method and High-Order SMC (HOSMC) to ensure the global stability of the control system. Thanks to this proposed method, the controller provides small position and velocity control errors with less oscillation, smooth control torque, and convergence of the control errors in the short time. The stability and convergence also are guaranteed with Lyapunov theory. Finally, computer simulation verifies the effectiveness of the designed controller.

INDEX TERMS Backstepping control, robotic manipulators, sliding mode control, global fast terminal sliding mode control, high-order sliding mode control.

I. INTRODUCTION

With the fast development of automation in the era of industry, robots are crucial for trade, engineering, medical, space, and ocean exploration, and so on [1]–[3]. To perform the tasks with high productivity or successful exploration, they should be controlled smoothly, safely, and reliably. Therefore, advanced robot controllers are demanded to provide high accuracy in various working conditions affected by the running environment such as external noise, measurement errors, or unknown uncertain components. In the literature, numerous methodologies have been introduced to deal with uncertainties, such as Computed Torque Control (CTC) [4], Adaptive Control [5], [6], Sliding Mode Control (SMC) [7], [8], PID Control [9], [10], Optimal Control [11], or some control methods [12]–[14]. In general, they have been verified to be efficient to handle simple uncertainties. For complex uncertain components, those methodologies only reduce the effects of uncertain components to a certain limit. Among those controllers, SMC has been widely used to deal with uncertainty and disturbance systems because of its usefulness such as strong robustness, easy implementation, design simplification [15]. The development of SMC method in theory and applications have been synthesized in document [16]. However, to solve a large uncertainty and disturbance, a large switching gain must be applied, which increases chattering behavior in control torque, the high friction between moving mechanical components, and generate high heat in the power circuit. Analysis of chattering has been shown at work of Arie Levant [17] or VI Utkin [18]. Besides that, SMC does not guarantee a predetermined convergence time, as well as had a worse transient response if the system is affected by the fast variation of disturbances. From the benefits and limitations of SMC, researchers are constantly developing to continue preserving the benefits and overcoming or eliminating the disadvantages of traditional SMC. First, in order to provide a finite-time convergence while enhancing the convergence characteristics of the dynamic system, some methods are known as Terminal Sliding Mode Control (TSMC) [19] and Fast Terminal SMC (FTSMC) [20] have been proposed. Compared to TSMC, FTSMC offers a faster convergence rate when the state error variables are far from the equilibrium point. However, traditional TSMC and FTSMC still have some disadvantages such as chattering component

The associate editor coordinating the review of this manuscript and approving it for publication was Mou Chen.

still exists in the control input as well as the singularity problem. To tackle this problem, a type of SMC technique called Nonsingular Fast Terminal SMC (NFTSMC) was developed [21]–[24]. NFTSMC has solved most of the problems, it provides a finite convergence time, fast convergence speed, avoiding singularity. Nonetheless, the oscillation behavior still appears in the control signal because the robust control law is still used to against the uncertain components. Second, to eliminate chattering, several techniques such as Boundary Layer Method (BLM) [25], Disturbance Observer [26], [27], Neural Network-based methods [28], [29], Adaptive Super-Twisting Method (ASTM) [30], Fuzzy- SMC (FSMC) [31], Second-Order SMC (SOSMC) [32], [33], or HOSMC [34] have been introduced. According to the level of effectiveness, HOSMC is more recommended because it generalizes the idea of the basic sliding mode acting on the higher-order derivative of system deviation instead of affecting the first derivation derivative as it happens in traditional SMC. So, HOSMC retains the original strong advantages of SMC, at the same time, they eliminate chattering phenomenon and providing greater accuracy in realization. Thirdly, to further increase the transient response of traditional SMC, some methods can be referred to as Integral SMC (ISMC) [35]–[37] or PID-SMC (PID-SMC) [38] has been proposed. In these proposals, the impact of the integral element in PID has been investigated, so this component is added to the sliding mode manifold to enhance transient response. Besides, Integral TSMC (ITSMC) has been proposed [39], [40], which provides a convergence in finite-time and fast transient response. However, traditional ITSMC still uses traditional Terminal sliding surface, leading to weaknesses of SMC still exist.

Recently, a few new approaches are based on intelligence computation [41]–[45], those have been widely applied to the tracking control of the robot manipulators with uncertain dynamics. With intelligent computational methods, the control systems can attain asymptotic stability. Moreover, several finite-time or fixed time control methods based on intelligent estimations have been suggested. However, the learning method always exists a problem in its implementation and it requires a very large calculation because of difficulty in training neural weight or setting fuzzy rules.

Based on the analysis mentioned above, to design a controller to continue to maintain the strengths of SMC and to thoroughly overcome the weaknesses of SMC at the same time. Therefore, this article is suggested. First, integral of the global fast terminal sliding mode surface has been developed, which provides a fast-transient response time and finite-time convergence and non-singular problem. In addition, the robot model is transferred into the third-order dynamic model according to the proposed sliding variable. Accordingly, an integral of the robust control law is derived, resulting in it providing a continuous signal at the control output like manner to HOSMC. Therefore, the proposed controller will provide several superior properties such as: strong robustness, fast finite-time convergence, fast transient response, and singularity avoidance. In addition, the proposed design procedure follows the backstepping control, thus, the overall stability of the system is secured according to Lyapunov criterion.

From technical and commercial perspectives, the controller for the robot manipulators should be low complicated, easy to implement in practice, and high effectiveness. In addition, considering the remarkable importance and advantages previously mentioned, a controller has been designed with the following notable contributions:

- The proposed method has values of NFTSMC, backstepping control method, and HOSMC. Its advantages, such as easy implementation, non-singularity, robustness in uncertainty elimination, high accuracy, fast transient response, and quick convergence in finite-time.
- Provides smooth control torque without chattering behavior when it uses an integral of the robust control method to tackle the influences of the uncertain components.
- The global stability of the control system is guaranteed by using the backstepping control method and Lyapunov theory.

The rest of this article has the following arrangement. Section 2 gives the issue formulations including presentation of the robot dynamic model and the goal of this article. Section 3 represents a synthesis of the proposed sliding surface and control design procedure. Continued after Section 3, two simulation examples are simulated to check for improved performance of the proposed controller when it is applied to a 2-DOF robot manipulator in Section 4. The control performance of the proposed system is then compared to the tracking control results of three other schemes, including CTC, SMC, and NFTSMC. The notable conclusions are given in Section 5.

II. PROBLEM STATEMENT

Based on [46], the robot dynamic model is formed by

$$\ddot{q} = M^{-1}(q)\left(\tau - C(q,\dot{q})\dot{q} - F(\dot{q}) - G(q) - \tau_d\right) \quad (1)$$

where $q \in \mathbb{R}^n$, $\dot{q} \in \mathbb{R}^n$ and $\ddot{q} \in \mathbb{R}^n$ represent the corresponding vector of position, velocity, and acceleration. $\tau \in \mathbb{R}^n$ is a control torque. $M(q) = \hat{M}(q) + \Delta M(q) \in \mathbb{R}^{n\times n}$ is the real inertia matrix, $C(q,\dot{q}) = \hat{C}(q,\dot{q}) + \Delta C(q,\dot{q}) \in \mathbb{R}^n$ denotes the real centrifugal and Coriolis forces, $G(q) = \hat{G}(q) + \Delta G(q) \in \mathbb{R}^n$ is the real gravitational forces matrix, $F(\dot{q}) \in \mathbb{R}^n$ is the frictional force, $\tau_d \in \mathbb{R}^n$ is disturbance force matrix. $\hat{M}(q) \in \mathbb{R}^{n\times n}$ represents the estimated inertia matrix, $\hat{C}(q,\dot{q}) \in \mathbb{R}^n$ represents the estimated centrifugal and Coriolis forces, $\hat{G}(q) \in \mathbb{R}^n$ stands for the estimated gravity. $\Delta M(q) \in \mathbb{R}^{n\times n}$, $\Delta C(q,\dot{q}) \in \mathbb{R}^n$ and $\Delta G(q) \in \mathbb{R}^n$ are the errors of dynamic model.

Therefore, the real robot dynamic model is represented by:

$$\ddot{q} = \hat{M}^{-1}(q)\left(\tau - \hat{C}(q,\dot{q})\dot{q} - \hat{G}(q) - \Delta\Theta\right) \quad (2)$$

where $\Delta\Theta = \Delta M(q)\ddot{q} + \Delta C(q,\dot{q})\dot{q} + \Delta G(q) + F(\dot{q}) + \tau_d$ is the vector of whole uncertain components, including external

disturbances, dynamic uncertainties, and estimated errors. For convenience and avoid repetition, we call these whole uncertain components as the lumped disturbance.

Define $x_1 = q$ and $x_2 = \dot{q}$, the dynamic equation (2) is transformed into a second-older state space model as follow:

$$\begin{cases} \dot{x}_1 = x_2 \\ \dot{x}_2 = b(x,t)u + f(x,t) + D \end{cases} \tag{3}$$

where $x = \begin{bmatrix} x_1{}^T & x_2{}^T \end{bmatrix}^T$ is a state vector, $u = \tau \in \mathbb{R}^n$ is a vector of the control input. $f(x,t) = \hat{M}^{-1}(q)\left(-\hat{C}(q,\dot{q})\dot{q} - \hat{G}(q)\right)$, $b(x,t) = \hat{M}^{-1}(q)$ and $D = -\hat{M}^{-1}(q)\,\Delta\Theta$.

Assumption 1: We assume that the whole uncertain components and its derivative are bounded by

$$\|D\| \leq \Xi \tag{4}$$

$$\left\| \frac{dD}{dt} \right\| \leq \Lambda \tag{5}$$

Remark 1: Assumptions in Eqs. (4)and (5) are the reality that has been verified in many published studies (readers can refer to the article [47], [48]).

In view of the basis TSMC theory, it is cleared that FTSMC contains many superior advantages, such as strong properties to uncertainties, non-singularity, finite-time convergence to the stable equilibrium, fast response time, and high accuracy. Therefore, we propose a backstepping global fast terminal sliding mode control for trajectory tracking control of industrial robotic manipulators in this article to overcome problems of TSMC with a combination of FTSMC, backstepping control, and HOSMC.

III. DESIGN OF BACKSTEPPING INTEGRAL FAST TERMINAL SLIDING MODE CONTROL

In this section, modification of the global FTSMS design has been proposed to obtain a fast-transient response, and finite-time convergence along with the system (3) is transformed into a third-order state-space model. Thanks to this technique, an integral of the robust reaching control law is found to reject the oscillation in the control torque, which is analyzed in more detail in the simulation section.

The tracking position and velocity errors are defined as:

$$\begin{aligned} x_{ei} &= x_{1i} - x_{di} \\ x_{dei} &= x_{2i} - \dot{x}_{di},\ i = 1, 2, \ldots, n \end{aligned} \tag{6}$$

where $x_d \in \mathbb{R}^n$ is the desired path vector.

With the control errors in Eq. (6), an IFTSM surface is proposed based on global FTSMS in reference [49] as follow:

$$s_i = \int \left(\begin{matrix} x_{dei} + \frac{2\alpha_1}{1+e^{-\beta_1(|x_{ei}|-\phi)}} x_{ei} \\ + \frac{2\alpha_2}{1+e^{\beta_2(|x_{ei}|-\phi)}} |x_{ei}|^{\kappa} sgn(x_{ei}) \end{matrix} \right), i = 1, 2, \ldots, n \tag{7}$$

where $s = \begin{bmatrix} s_1 & s_2 & \ldots & s_n \end{bmatrix}^T$ is the sliding mode vector, $\alpha_1, \alpha_2, \beta_1, \beta_2$ stand for the positive coefficients, $0 < \kappa < 1$, and $\phi = \left(\frac{\alpha_2}{\alpha_1}\right)^{1/(1+\kappa)}$.

According to the theory of sliding motion [50], the conditions for sliding motion must meet the following requirements

$$\begin{aligned} s_i &= 0; \\ \dot{s}_i &= 0 \end{aligned} \tag{8}$$

Combining the proposed sliding surface in Eq. (7) with the conditions of the sliding motion in Eq. (8), we can gain

$$\begin{aligned} x_{dei} = &-\frac{2\alpha_1}{1+e^{-\beta_1(|x_{ei}|-\phi)}} x_{ei} \\ &- \frac{2\alpha_2}{1+e^{\beta_2(|x_{ei}|-\phi)}} |x_{ei}|^{\kappa} sgn(x_{ei}) \end{aligned} \tag{9}$$

To prove the correctness of the finite-time convergence, let us consider a Lyapunov candidate as follows

$$V = 0.5 x_{ei}^2 \tag{10}$$

Differentiating Eq. (10) with respect to time obtains

$$\begin{aligned} \dot{V} &= x_{ei} x_{dei} \\ &= -\frac{2\alpha_1}{1+e^{-\beta_1(|x_{ei}|-\phi)}} |x_{ei}| - \frac{2\alpha_2}{1+e^{\beta_2(|x_{ei}|-\phi)}} |x_{ei}|^{\kappa+1} < 0 \end{aligned} \tag{11}$$

According to inequality (11), it is clear that $V > 0$ and $\dot{V} < 0$. Therefore, the position and velocity control errors will converge to the equilibrium point.

When $|x_{ei}| > \phi$, the sliding motion consists of two stages: $x_{ei}(0) \rightarrow |x_{ei}| = \phi$ and $|x_{ei}| = \phi \rightarrow x_{ei} = 0$. The convergence time of two phases is calculated as follows:

In the first stage, the first component represents the main role. Therefore, the convergence time in this period is calculated by:

$$\begin{aligned} \int_0^{t_1} dt = &\int_{x_{ei}(0)}^{\phi} \frac{1}{-\frac{2\alpha_1}{1+e^{-\beta_1(|e_i|-\phi)}} |x_{ei}| - \frac{2\alpha_2}{1+e^{\beta_2(|e_i|-\phi)}} |x_{ei}|^{\kappa+1}} \\ &\times d(|x_{ei}|) < \int_{\phi}^{x_{ei}(0)} \frac{1}{\alpha_1 |x_{ei}|} d(|x_{ei}|) \end{aligned} \tag{12}$$

Then,

$$t_1 < \frac{\ln(|x_{ei}(0)|) - \ln(\phi)}{\alpha_1} \tag{13}$$

In the second stage, the second component plays the main role. Therefore, the convergence time in this period is computed as follows:

$$\begin{aligned} \int_0^{t_2} dt &= \int_{\phi}^{0} \frac{1}{-\frac{2\alpha_1}{1+e^{-\beta_1(|e_i|-\phi)}} |x_{ei}| - \frac{2\alpha_2}{1+e^{\beta_2(|e_i|-\phi)}} |x_{ei}|^{\kappa+1}} d(|x_{ei}|) \\ &= \int_0^{\phi} \frac{1}{\frac{2\alpha_1}{1+e^{-\beta_1(|e_i|-\phi)}} |x_{ei}| + \frac{2\alpha_2}{1+e^{\beta_2(|e_i|-\phi)}} |x_{ei}|^{\kappa+1}} d(|x_{ei}|) \\ &< \int_0^{\phi} \frac{1}{\alpha_2 |x_{ei}|^{\kappa}} d(|x_{ei}|) \end{aligned} \tag{14}$$

Then,

$$t_2 < \frac{1}{\alpha_2}\left(\frac{\phi^{1-\kappa}}{1-\kappa}\right) \tag{15}$$

Consequently, Therefore, the total time of the sliding motion ($x_{ei}(0) \to 0$) is calculated by:

$$t_s = t_1 + t_2 < \frac{\ln(|x_{ei}(0)|) - \ln(\phi)}{\alpha_1} + \frac{1}{\alpha_2}\left(\frac{\phi^{1-\kappa}}{1-\kappa}\right) \tag{16}$$

With the analysis of the role of each term in Eq. (9) from Eqs. (12) - (16), it is concluded that the core idea of this approach is to increase the influence of the term that plays a major role while reducing the influence of the minor term at the same time, which has a great contribution to enhancing the control system's response performance.

The first and second derivative of the sliding surface is correspondingly computed as follows:

$$\begin{aligned}\dot{s}_i = {} & x_{dei} + \frac{2\alpha_1}{1+e^{-\beta_1(|x_{ei}|-\phi)}}x_{ei} \\ & + \frac{2\alpha_2}{1+e^{\beta_2(|x_{ei}|-\phi)}}|x_{ei}|^{\kappa} sgn(x_{ei}), \quad i = 1, 2, 3, \ldots, n\end{aligned} \tag{17}$$

$$\begin{aligned}\ddot{s}_i = {} & \dot{x}_{dei} + \frac{2\alpha_1}{1+e^{-\beta_1(|x_{ei}|-\phi)}}x_{dei} \\ & + \frac{2\alpha_1\beta_1 x_{dei} sgn(x_{ei}) e^{-\beta_1(|x_{ei}|-\phi)}}{\left(1+e^{-\beta_1(|x_{ei}|-\phi)}\right)^2}x_{ei} \\ & + \frac{2\alpha_2\kappa}{1+e^{\beta_2(|x_{ei}|-\phi)}}|x_{ei}|^{\kappa-1}x_{dei} \\ & - \frac{2\alpha_2\beta_2 x_{dei} e^{\beta_2(|x_{ei}|-\phi)}}{\left(1+e^{\beta_2(|x_{ei}|-\phi)}\right)^2}|x_{ei}|^{\kappa}, \quad i = 1, 2, 3, \ldots, n\end{aligned} \tag{18}$$

To simplify, let

$$\begin{aligned}Z_i = {} & \frac{2\alpha_1}{1+e^{-\beta_1(|x_{ei}|-\phi)}}x_{dei} \\ & + \frac{2\alpha_1\beta_1 x_{dei} sgn(x_{ei}) e^{-\beta_1(|x_{ei}|-\phi)}}{\left(1+e^{-\beta_1(|x_{ei}|-\phi)}\right)^2}x_{ei} \\ & + \frac{2\alpha_2\kappa}{1+e^{\beta_2(|x_{ei}|-\phi)}}|x_{ei}|^{\kappa-1}x_{dei} \\ & - \frac{2\alpha_2\beta_2 x_{dei} e^{\beta_2(|x_{ei}|-\phi)}}{\left(1+e^{\beta_2(|x_{ei}|-\phi)}\right)^2}|x_{ei}|^{\kappa}, \quad i = 1, 2, 3, \ldots, n\end{aligned} \tag{19}$$

Therefore, the matrix form of Eq. (18) is expressed as:

$$\ddot{s} = \dot{x}_{de} + Z \tag{20}$$

where $Z = \begin{bmatrix} Z_1 & Z_2 & \ldots & Z_n \end{bmatrix}^T \in \mathbb{R}^{n\times 1}$.

Based on dynamic model of Eq. (3), the first derivation of the sliding surface in (17) and the second derivation of Eq. (20), the dynamic system (3) is transformed in to the third-order state space model according to IFTSM surface as

$$\begin{cases} s_1 = s \\ \dot{s}_1 = s_2 \\ \dot{s}_2 = s_3 \\ \dot{s}_3 = \frac{d}{dt}\left(b(x,t)u + f(x,t) + D - \ddot{x}_d + Z\right) \end{cases} \tag{21}$$

In order to achieve the effective control torque for dynamic system in Eq. (21), a backstepping design approach is proposed. Therefore, the following change of coordinate is launched:

$$\vartheta_1 = [\vartheta_{11} \quad \vartheta_{12} \quad \ldots \quad \vartheta_{1n}]^T = s_1 \in \mathbb{R}^{n\times 1} \tag{22}$$

$$\vartheta_2 = [\vartheta_{21} \quad \vartheta_{22} \quad \ldots \quad \vartheta_{2n}]^T = s_2 - \varsigma_1 \in \mathbb{R}^{n\times 1} \tag{23}$$

$$\vartheta_3 = [\vartheta_{31} \quad \vartheta_{32} \quad \ldots \quad \vartheta_{3n}]^T = s_3 - \varsigma_2 \in \mathbb{R}^{n\times 1} \tag{24}$$

where $\varsigma_1 \in \mathbb{R}^{n\times 1}$ and $\varsigma_2 \in \mathbb{R}^{n\times 1}$ are the virtual control laws in the first and second steps, respectively.

In addition, to prove global asymptotic stability of the designed control strategy, the proof procedure will be conducted in the following 3 steps

Step 1: the target of this step is to design a virtual control input ς_1 which drives $\vartheta_1 \to 0$. Therefore, Lyapunov candidate is selected as

$$V_1 = 0.5\vartheta_1{}^T\vartheta_1 \tag{25}$$

Differentiating ϑ_1 in Eq. (22) with respect to time yields

$$\dot{\vartheta}_1 = \dot{s}_1 = s_2 = \vartheta_2 + \varsigma_1 \tag{26}$$

and differentiating V_1 in Eq. (25) with respect to time and using Eq. (26) gains

$$\dot{V}_1 = \vartheta_1{}^T\dot{\vartheta}_1 = \vartheta_1{}^T(\vartheta_2 + \varsigma_1) \tag{27}$$

Virtual control ς_1 is appropriately selected to make the first-order system stabilizable.

$$\varsigma_1 = -\xi_1\vartheta_1 \tag{28}$$

where ξ_1 is design parameter which is assigned as positive constant.

Substituting (28) into (27) obtains

$$\dot{V}_1 = \vartheta_1{}^T\vartheta_2 - \xi_1\sum_{i=1}^{n}\vartheta_{1i}{}^2 \tag{29}$$

According to Eq. (29), we can observe that if $\vartheta_2 = 0$ then $\dot{V}_1 = -\xi_1\sum_{i=1}^{n}\vartheta_{1i}{}^2 \le 0$. Consequently, ϑ_1 will be asymptotically stable.

Step 2: the purpose of this step is to generate a virtual control input ς_2 which drives an error variable $\vartheta_2 \to 0$. Choose a control Lyapunov function as:

$$V_2 = V_1 + 0.5\vartheta_2{}^T\vartheta_2 \tag{30}$$

Differentiating ϑ_2 in Eq. (23) with respect to time archives

$$\begin{aligned}\dot{\vartheta}_2 &= \dot{s}_2 - \dot{\varsigma}_1 \\ &= \vartheta_3 + \varsigma_2 - \dot{\varsigma}_1 \\ &= \vartheta_3 + \varsigma_2 + \xi_1 s_2\end{aligned} \tag{31}$$

Differentiating V_2 in Eq. (30) with respect to time and using Eq. (31) gains

$$\begin{aligned}\dot{V}_2 &= \dot{V}_1 + \vartheta_2{}^T\dot{\vartheta}_2 \\ &= -\xi_1\sum_{i=1}^{n}\vartheta_{1i}{}^2 + \vartheta_1{}^T\vartheta_2 + \vartheta_2{}^T(\vartheta_3 + \varsigma_2 + \xi_1 s_2)\end{aligned} \tag{32}$$

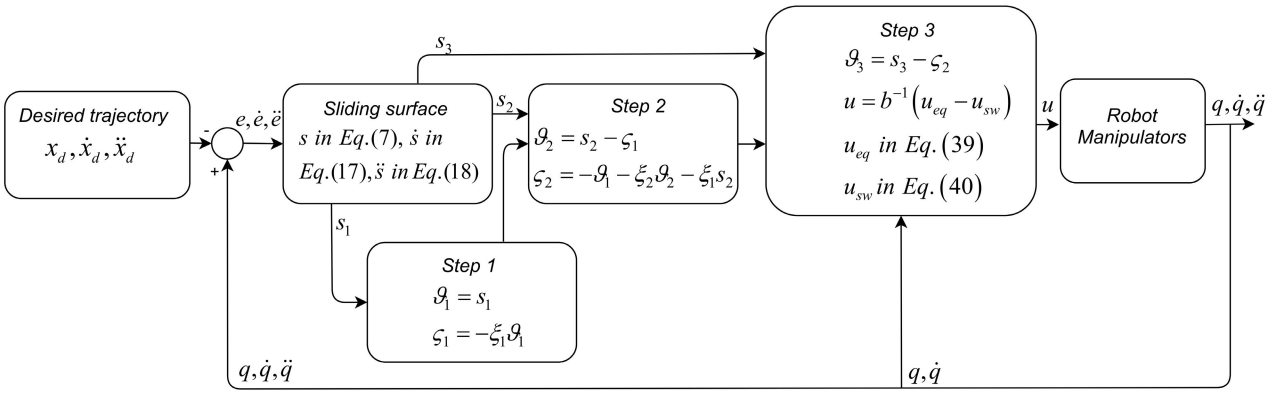

FIGURE 1. Proposed BIFTSMC scheme.

Based on (32), the virtual control is appropriately chosen to eliminate terms related to ϑ_1 and s_2, while the term involving ϑ_3 cannot be eliminated

$$\varsigma_2 = -\vartheta_1 - \xi_2\vartheta_2 - \xi_1 s_2 \tag{33}$$

Substituting (33) into (32) obtains

$$\begin{aligned}\dot{V}_2 &= -\xi_1 \sum_{i=1}^{n} {\vartheta_{1i}}^2 + {\vartheta_1}^T \vartheta_2 \\ &\quad + {\vartheta_2}^T (\vartheta_3 - \vartheta_1 - \xi_2\vartheta_2 - \xi_1 s_2 + \xi_1 s_2) \\ &= -\xi_1 \sum_{i=1}^{n} {\vartheta_{1i}}^2 - \xi_2 \sum_{i=1}^{n} {\vartheta_{2i}}^2 + {\vartheta_2}^T \vartheta_3 \end{aligned} \tag{34}$$

From the result in Eq. (34), $\dot{V}_2 = -\xi_1 \sum_{i=1}^{n} {\vartheta_{1i}}^2 - \xi_2 \sum_{i=1}^{n} {\vartheta_{2i}}^2 \leq 0$ can be obtained once $\vartheta_3 = 0$. Consequently, the state ϑ_1 and ϑ_2 will be asymptotically stable.

Step 3: the aim of this step is to propose the real control torque u which controls ϑ_1, ϑ_2, ϑ_3 to zero. Consider the following Lyapunov function:

$$V_3 = V_2 + 0.5{\vartheta_3}^T \vartheta_3 \tag{35}$$

Differentiating V_3 with respect to time yields

$$\dot{V}_3 = \dot{V}_2 + {\vartheta_3}^T \dot{\vartheta}_3 \tag{36}$$

Substituting the Eqs. (21), (24) and (34) into Eq. (36), we have

$$\begin{aligned}\dot{V}_3 &= -\xi_1 \sum_{i=1}^{n} {\vartheta_{1i}}^2 - \xi_2 \sum_{i=1}^{n} {\vartheta_{2i}}^2 + {\vartheta_2}^T \vartheta_3 \\ &\quad + {\vartheta_3}^T \left(\frac{d}{dt} (b(x,t)u + f(x,t) + D - \ddot{x}_d + Z) - \dot{\varsigma}_2 \right) \end{aligned} \tag{37}$$

Therefore, a backstepping IFTSMC (BIFTSMC) is designed as

$$u = b^{-1}(x,t) \left(u_{eq} - u_{sw} \right) \tag{38}$$

where

$$u_{eq} = -Z - f(x,t) + \ddot{x}_d + \varsigma_2 - \int (\xi_3\vartheta_3 + \vartheta_2) \tag{39}$$

and the reaching control law is introduced by

$$\dot{u}_{sw} = (\Lambda + \nu)\, sgn(\vartheta_3) \tag{40}$$

where ν is a small positive constant.

The block diagram of the proposed controller is described in Fig. 1

Applying the designed controller in Eqs. (38) - (40) to Eq. (37) yields

$$\begin{aligned}\dot{V}_3 &= -\xi_1 \sum_{i=1}^{n} {\vartheta_{1i}}^2 - \xi_2 \sum_{i=1}^{n} {\vartheta_{2i}}^2 \\ &\quad -\xi_3 \sum_{i=1}^{n} {\vartheta_{3i}}^2 + {\vartheta_3}^T \frac{d}{dt} (-u_{sw} + D) \\ &= -\xi_1 \sum_{i=1}^{n} {\vartheta_{1i}}^2 - \xi_2 \sum_{i=1}^{n} {\vartheta_{2i}}^2 \\ &\quad -\xi_3 \sum_{i=1}^{n} {\vartheta_{3i}}^2 - (\Lambda + \nu)\, {\vartheta_3}^T sgn(\vartheta_3) + {\vartheta_3}^T \frac{dD}{dt} \\ &\leq -\xi_1 \sum_{i=1}^{n} {\vartheta_{1i}}^2 - \xi_2 \sum_{i=1}^{n} {\vartheta_{2i}}^2 \\ &\quad -\xi_3 \sum_{i=1}^{n} {\vartheta_{3i}}^2 - (\Lambda + \nu) \sum_{i=1}^{n} |\vartheta_{3i}| + \Lambda \sum_{i=1}^{n} |\vartheta_{3i}| \\ &\leq -\xi_1 \sum_{i=1}^{n} {\vartheta_{1i}}^2 - \xi_2 \sum_{i=1}^{n} {\vartheta_{2i}}^2 \\ &\quad -\xi_3 \sum_{i=1}^{n} {\vartheta_{3i}}^2 - \nu \sum_{i=1}^{n} |\vartheta_{3i}| \end{aligned} \tag{41}$$

Then, $\dot{V}_3 \leq 0$, $\dot{V}_3$ is a negative semidefinite, it is mean that ϑ_1, ϑ_2 and ϑ_3 will converge to zero in a finite time.

IV. VALIDATION AND DISCUSSION

To verify the performance of the proposed controller, we employ it for a 2-DOF robotic manipulator. Firstly, all the mechanic parts of 2-DOF robotic manipulator was designed in SOLIDWORKS. Secondly, these mechanic parts were introduced into the SolidWorks assembly environment to attach the coordinate system, complete assembly, and determine the direction of gravity. Thirdly, after completing the assembly of the 2-DOF robotic manipulator model, using the Simscape Multibody Link Tool in SOLIDWORKS that assembly model is exported to an XML file and STEP files. Where, the XML file contains all parameters of the mechanical parts of the robot such as mass, inertia moment, the center of mass, and all parameters of the coordinate system of the assembly environment, STEP files contain a 3D shape of the mechanical parts of the robot. Finally, XML file and STEP files are imported into the MATLAB/SIMULINK environment by using the Simscape Multibody Link tool of MATLAB. By using this way, the mechanical model of

the 2-DOF robotic manipulator is completely identical to the actual model. Disturbance and friction components have added to the system. 2-DOF robotic mechanical model in SOLIDWORKS is shown in Fig. 2 and its parameters are given in Table 1.

FIGURE 2. 2-DOF robotic mechanical model in SOLIDWORKS.

TABLE 1. The parameter of 2-DOF robotic manipulator.

	Link 1	Link 2
Length (m)	0.3	0.3
Weight (kg)	11.941	7. 401
Center of mass (m)	0.193	0.154
Inertia $(kg.m^2)$	$150901.5816 \times 10^{-6}$	$78091.7067 \times 10^{-6}$

In the MATLAB/SIMULINK environment, the configuration of the model is set under a fixed-step (ODE5 dormand-prince) with a fundamental sample time of 0.001 seconds.

To test the advanced capabilities and outstanding efficiency of the proposal system. The designed control system applies to the aforementioned robotic manipulator and its control performance is compared with CTC, SMC and NFTSMC.

The CTC has the following control torque

$$u = b^{-1}(x,t)\left(-f(x,t) + \ddot{x}_d - K_p x_e - K_d x_{de}\right) \quad (42)$$

where K_p and K_d are positive constants.

The control torque of the conventional SMC is proposed as follows:

$$u = b^{-1}(x,t)\left(-f(x,t) + \ddot{x}_d - c x_{de} - (\Xi + \nu)\, sgn(s)\right) \quad (43)$$

where $s = x_{de} + c x_e$ with c is a positive constant. ν is a small positive coefficient.

The control torque of NFTSMC is designed as

$$u = b^{-1}(x,t)\left(u_{eq} - u_{sw}\right) \quad (44)$$

where

$$u_{eq} = -\left(f(x,t) - \ddot{x}_d\right) - \varphi^{-1}(x_{de})\Gamma(x_e, x_{de}) \quad (45)$$

$$u_{sw} = (\Xi + \nu)\, sgn(s) \quad (46)$$

and

$$s = x_e + a_1 x_e^{[b_1]} + a_2 x_{de}^{[b_2]} \quad (47)$$

$$\varphi(x_{de}) = a_2 b_2 |x_{de}|^{b_2 - 1} \quad (48)$$

$$\Gamma(x_e, x_{de}) = x_{de} + a_1 b_1 |x_e|^{b_1 - 1} x_{de} \quad (49)$$

where a_1, a_2, b_1, b_2 are positive constants and ν is a small positive coefficient.

The desired trajectory of a robot's end-effector is designed to track the following circle:

$$\begin{cases} X_d = 0.3 + 0.05\cos(t) \\ Y_d = 0.15 + 0.05\sin(t) \end{cases} \quad (50)$$

In order to investigate the position tracking accuracy and to facilitate the evaluation, tracking errors are considered after the period of convergence around the equilibrium point and maintaining stable accuracy. Accuracy review time is $t = 1s \rightarrow 15s$, the control errors are calculated by Eq. (51), and the results are reported in Table 3 and 5.

$$e_x = \sqrt{\frac{1}{N}\sum_{i=1}^{N}(X_{di} - x_i)^2},\ e_y = \sqrt{\frac{1}{N}\sum_{i=1}^{N}(Y_{di} - y_i)^2}$$
$$e_1 = \sqrt{\frac{1}{N}\sum_{i=1}^{N}(q_{1di} - q_{1i})^2},\ e_2 = \sqrt{\frac{1}{N}\sum_{i=1}^{N}(q_{2di} - q_{2i})^2} \quad (51)$$

where N is the number of considered samples. X_{di}, Y_{di} and x, y stand for the assigned path and the real path of the robot's end-effector at the time index i respectively. q_{1di}, q_{2di} and q_{1i}, q_{2i} are the desired angle of the joint and the actual angle of joint at time index respectively.

Moreover, to investigate advanced abilities of the proposed scheme, we proceed to apply the controllers, including CTC, SMC, NFTSMC, and the proposed control scheme to the above robotic manipulators in the two following cases:

A. CASE 1

We seem to have an exact dynamic model of the robot, that means the errors of dynamic model $\Delta M(q) = 0$, $\Delta C(q, \dot{q}) = 0$, and $\Delta G(q) = 0$. Therefore, we only consider the effects of the following friction and external disturbance.

Friction term was modeled as

$$F(\dot{q}) = \begin{bmatrix} -0.5\sin(\dot{q}_1) - 0.5\dot{q}_1 \\ -0.1\sin(\dot{q}_2) - 0.5\dot{q}_2 \end{bmatrix} \quad (52)$$

and external disturbances:

$$\tau_d(t) = \begin{bmatrix} 3\sin(t) \\ \sin(t) \end{bmatrix} \quad (53)$$

The control parameters of four different controllers for case 1 are shown in table 2.

The tracking simulation results of all 4 control methods, including CTC, SMC, NFTSMC, and BIFTMC for a two-DOF robot are indicated in Figs. 3-10. The designed trajectory and actual trajectory of the four control methods

TABLE 2. The control parameters of four different controllers for case 1.

Control Methods	Parameters	Value
CTC	k_P, k_D	$500, 50$
SMC	c, Ξ, ν	$5, 7, 0.1$
NFTSMC	$a_1, a_2, b_1, b_2, \Xi, \nu$	$10, 1.5, 1.7, 5/3, 7, 0.1$
Proposed controller (BIFTSMC)	$\alpha_1, \alpha_2, \beta_1, \beta_2, \kappa, \Lambda, \nu$	$10, 7, 5, 0.3, 0.8, 7, 0.1$
	ξ_1, ξ_2, ξ_3	$40, 40, 40$

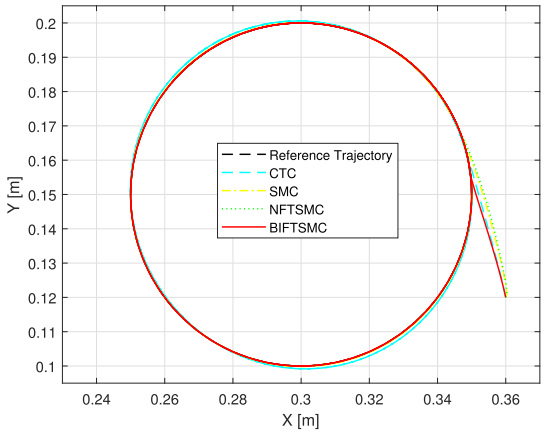

FIGURE 3. Assigned path and actual path of the robot's end-effector under four algorithms.

in tracking the orbital circle are shown in Fig. 3. From simulated performance, it is observed that those four control schemes controlled the robot manipulator to track the assigned path under the assumed friction and disturbances. To compare in detail, we can clearly see from Figs. 4-7, CTC provides the worst control errors among 4 control systems at the two joints 0.0014204 and 0.0018633, respectively, as well as position control errors of the end-effector are corresponding to 0.00076694 (in X-Direction) and 0.00049986 (in Y-Direction). SMC provides control errors smaller than CTC at the two joints 0.00027125 and 0.00028427, respectively, as well as position control errors of the end-effector are corresponding to 0.00012397 (in X-Direction) and 9.1699×10^{-5} (in Y-Direction), respectively. However, it provides worse control errors than NFTSMC, NFTSMC has the control errors at the two joints 2.3488×10^{-5} and 3.1090×10^{-5}, respectively, as well as the tracking errors of the end-effector are corresponding to 1.2636×10^{-5} (in X-Direction) and 8.1973×10^{-6} (in Y-Direction), respectively. It is worth noting that BIFTMC has the smallest control errors among 4 control systems at the two joints 3.8056×10^{-8} and 3.9500×10^{-8}, respectively, as well as position control errors of the end-effector are corresponding to 1.3539×10^{-8} (in X-Direction) and 1.1844×10^{-8} (in Y-Direction), respectively. In addition, BIFTMC has the smallest convergence time and highest accuracy.

Special points need attention from the tracking velocity in Figs. 8 and 9 (we only consider methods based on SMC and TSMC), it is seen that both SMC and NFTSMC have the tracking velocity errors with oscillation in their velocity outputs. While velocity outputs provided by the designed controller have minor oscillation.

TABLE 3. The root mean square of path control errors of four algorithms of case 1.

Control Methods	e_x (X-Deriection)	e_y (Y-Deriection)	e_1 (Joint 1)	e_2 (Joint 2)
CTC	0.00076694	0.00049986	0.0014204	0.0018633
SMC	0.00012397	9.1699×10^{-5}	0.00027125	0.00028427
NFTSMC	1.2636×10^{-5}	8.1973×10^{-6}	2.3488×10^{-5}	3.1090×10^{-5}
Proposed controller (BIFTSMC)	1.3539×10^{-8}	1.1844×10^{-8}	3.8056×10^{-8}	3.9500×10^{-8}

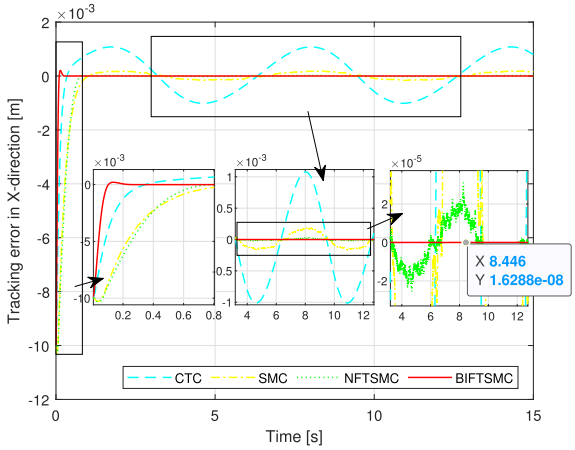

FIGURE 4. Position control error of the robot's end-effector in X-direction.

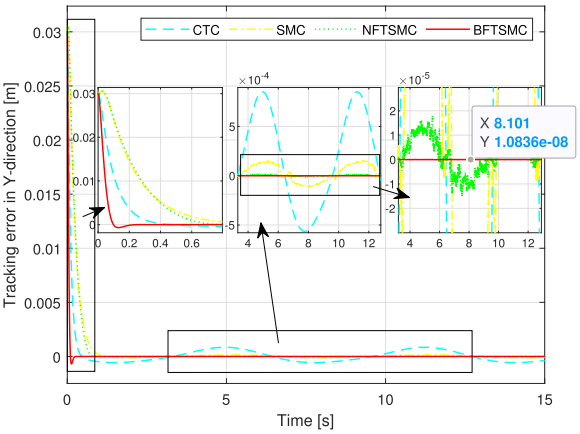

FIGURE 5. Position control error of the robot's end-effector in Y-direction.

Control input signals of the four separate control systems at first joint and second joint are exhibited in Fig. 10. We realize that SMC and NFTSMC provide discontinuous control torque when both methods use a large sliding gain in the reaching control law to compensate for the effects of the uncertain components. Specifically, the upper limit value of the uncertain components must be determined. Obviously, CTC and BIFTSMC provide smooth control signals. BIFTSMC can obtain this target because its high-frequency control law used an integral of the control torque as shown in Eq. (40).

B. CASE 2

We consider an uncertain robot manipulator, in which we assumed that the errors of dynamic model $\Delta M(q) = 0.3M(q)$, $\Delta C(q, \dot{q}) = 0.3C(q, \dot{q})$, and $\Delta G(q) = 0.3G(q)$.

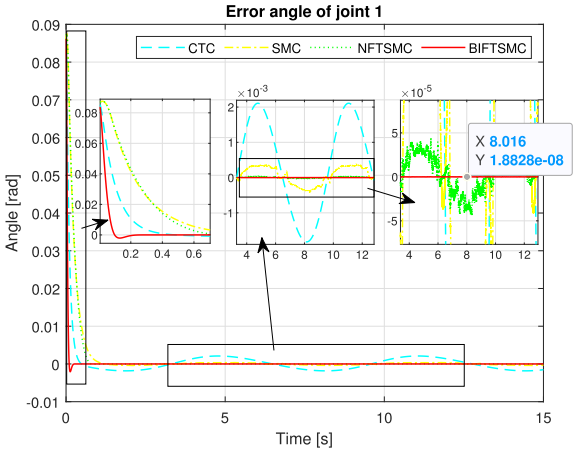

FIGURE 6. Position control errors of joint 1.

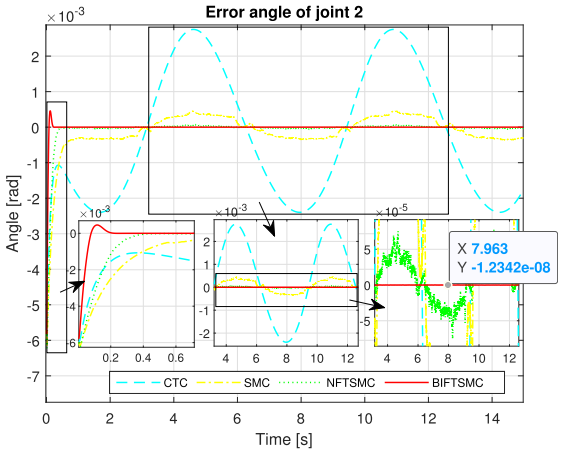

FIGURE 7. Position control errors of joint 2.

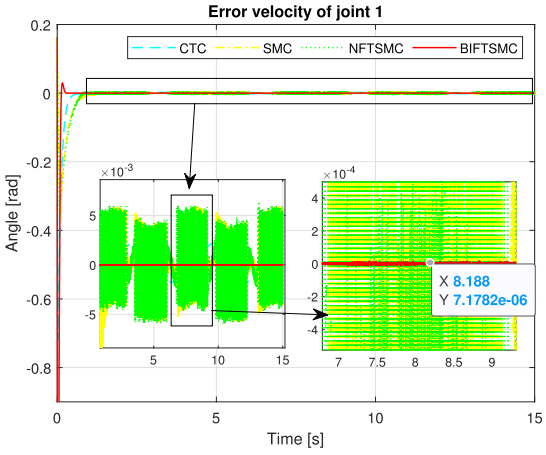

FIGURE 8. Velocity control errors of joint 1.

This example is more like a real-world system because it is difficult to achieve a precise dynamic. The effects of the considered friction and external disturbance are given in Eqs. (52) and (53).

The control parameters of four different controllers for case 2 are shown in Table 4.

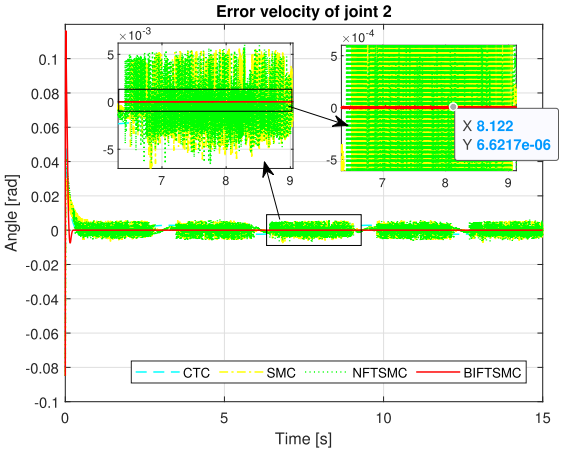

FIGURE 9. Velocity control errors of joint 2.

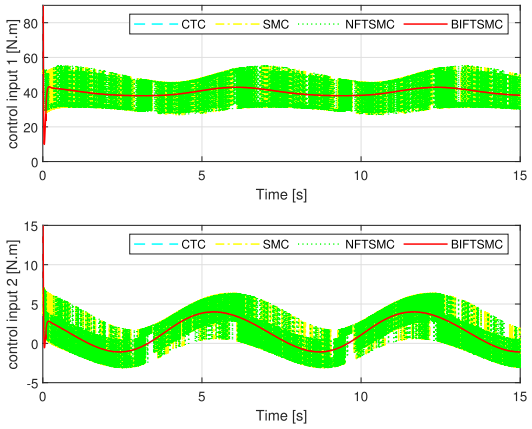

FIGURE 10. Control inputs at joint 1 and joint 2.

TABLE 4. The control parameters of four different controllers for case 2.

Control Methods	Parameters	Value
CTC	k_P, k_D	$1000, 100$
SMC	$c,\ \Xi,\ \nu$	$5, 18, 0.1$
NFTSMC	$a_1, a_2, b_1, b_2, \Xi, \nu$	$10, 1.5, 1.7, 5/3, 18, 0.1$
Proposed controller (BIFTSMC)	$\alpha_1, \alpha_2, \beta_1, \beta_2, \kappa,\ \Lambda, \nu$	$10, 7, 5, 0.3, 0.8, 18, 0.1$
	ξ_1, ξ_2, ξ_3	$40, 40, 40$

Simulation results for an uncertain robot system are shown in Figs. 11-18. From Figs. 11-17 and Table 5, we realize that the control performance provided by the CTC is severely reduced when it is not able to compensate for the influence of uncertain dynamic components. The tracking accuracy of CTC is highly dependent on the exact robot dynamic model. The accuracy and speed of convergence provided by SMC or NFTSMC are also reduced. To compensate for those declines, the sliding values of the robust control law must be accordingly increased, hence, more chattering is generated in their control outputs. Compared to the chattering results in Fig. 10 and Fig. 18, it is seen that chattering behavior has increased significantly. This may the undesired vibrations in the robot system and cause damage to the system. Fortunately, the performance of the proposed controller, including position tracking accuracy and convergence speed, is not reduced.

TABLE 5. The root mean square of path control errors of four algorithms of case 2.

Control Methods	e_x (X-Deriection)	e_y (Y-Deriection)	e_1 (Joint 1)	e_2 (Joint 2)
CTC	0.00141920	0.00384020	0.01282800	0.00678010
SMC	0.00012003	0.00026035	0.00086690	0.00059516
NFTSMC	2.1941×10^{-5}	4.2124×10^{-5}	0.00014281	0.00010548
Proposed controller (BIFTSMC)	2.5267×10^{-8}	1.5498×10^{-8}	5.0069×10^{-8}	8.0307×10^{-8}

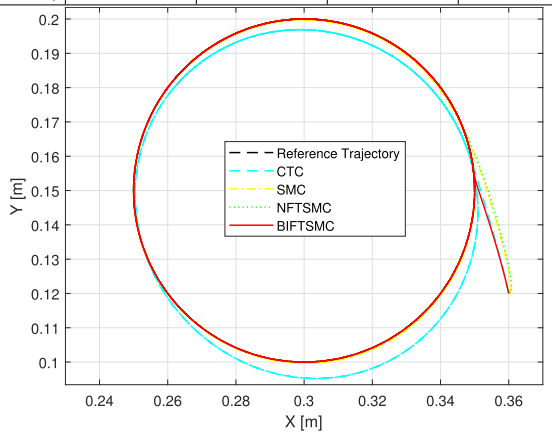

FIGURE 11. Assigned path and actual path of the robot's end-effector under four algorithms.

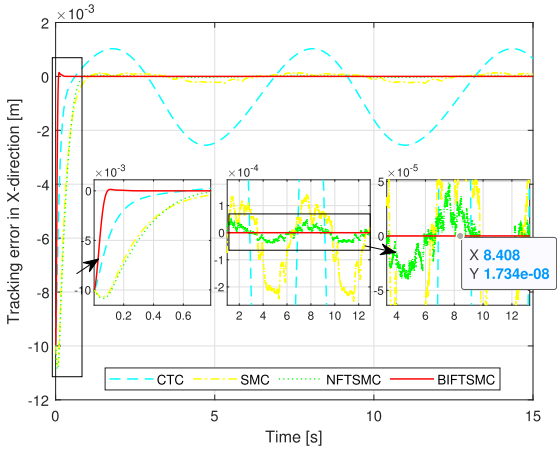

FIGURE 12. Position tracking error of the robot's end-effector in X-direction.

The proposed controller still provides the best control performance among the compared control methods and no chattering behavior occurs in its control input. From two simulation cases, it can be concluded that the proposed controller shows superiority over the other three methods, such as smooth control inputs, robustness in uncertainty elimination, higher accuracy, and faster finite-time convergence.

Remark 2: The authors think that the limitation of our control method is that the upper bound value of the derivative of the whole uncertain components needs to know in advance. However, this problem is not difficult to solve. The upper bound value of the whole uncertain components can be obtained by using adaptive techniques [51], [52] to adapt to the variation of the uncertainties.

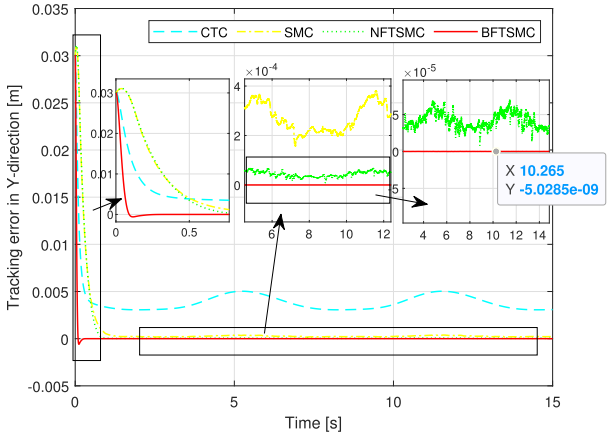

FIGURE 13. Position tracking error of the robot's end-effector in Y-direction.

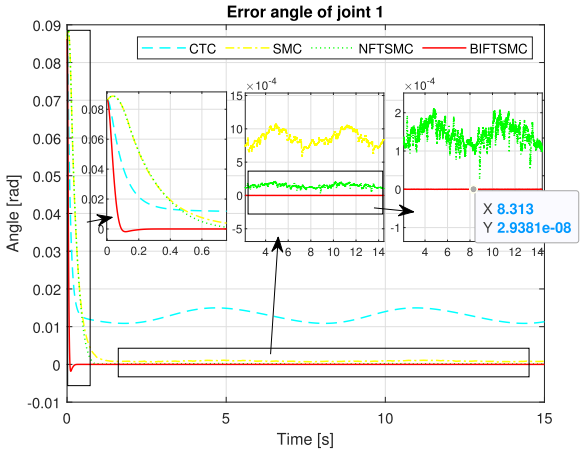

FIGURE 14. Position control errors of joint 1.

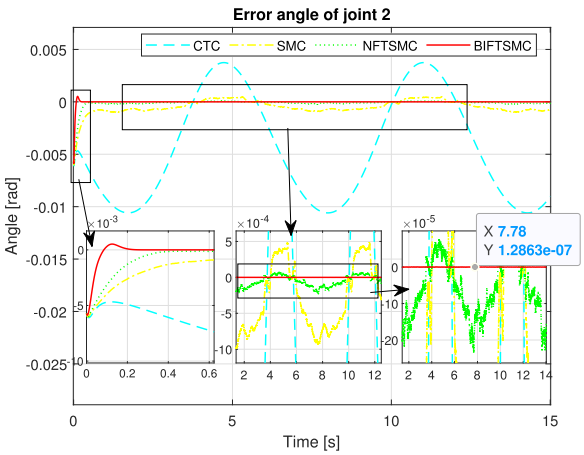

FIGURE 15. Position control errors of joint 2.

Remark 3: There are some control methods to improve the control performance by using an observer. Using the control combined with an observer has confirmed that it will be provided a better tracking performance than a controller without an observer. That is also our research orientation in the next works.

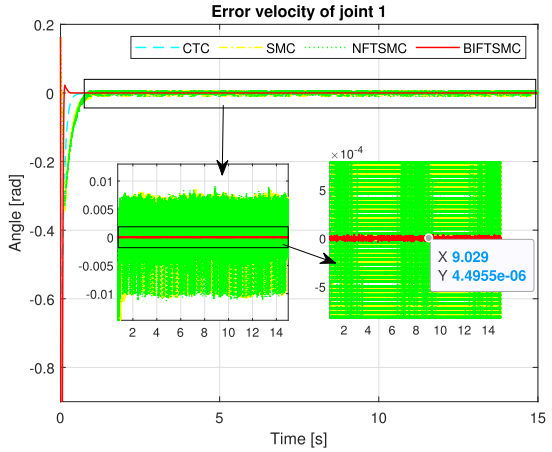

FIGURE 16. Velocity control errors of joint 1.

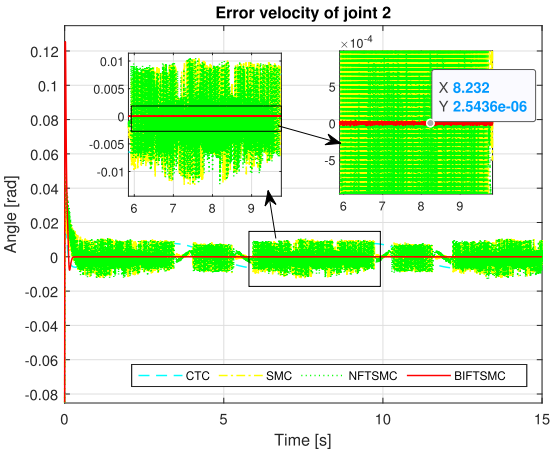

FIGURE 17. Velocity control errors of joint 2.

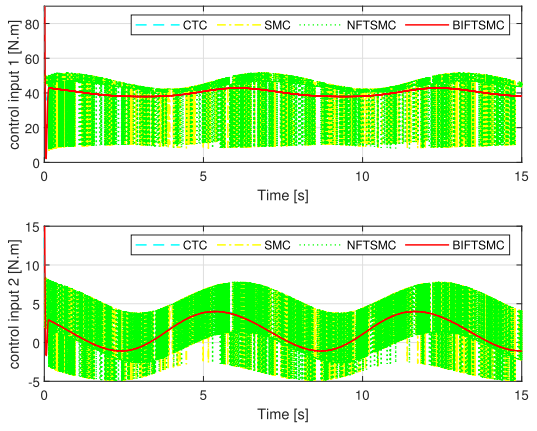

FIGURE 18. Control inputs at joint 1 and joint 2.

V. CONCLUSION

We propose a backstepping global fast terminal sliding mode control for trajectory tracking control of industrial robotic manipulators in this article. An integral of the global fast terminal sliding mode surface is firstly suggested to improve the dynamic performance and fast convergence of SMC and TSMC, which also obtains a finite-time convergence. A controller is later developed from the proposed sliding surface using the backstepping control method and High-Order SMC to ensure the global stability of the control system. Thanks to this proposed method, the controller provides small position and velocity control errors with less oscillation, smooth control torque, and convergence of the control errors in the short time. The stability and convergence also are guaranteed with Lyapunov theory. Finally, computer simulation verifies the effectiveness of the designed controller.

From verification by computer simulation results it is noticed that 1) the proposed method has values of NFTSMC, backstepping control method, and HOSMC. Its advantages, such as easy implementation, non-singularity, robustness in uncertainty elimination, high accuracy, fast transient response, and quick convergence in finite-time; 2) provides smooth control torque without chattering behavior when it uses an integral of the high-frequency control law to tackle the influences of the uncertain components.

VI. FUTURE WORK

The next target is to apply the proposed control system for a real robot manipulator.

REFERENCES

[1] K. De Backer *et al.*, "Industrial robotics and the global organisation of production," OECD Sci., Technol. Ind., OECD Publishing, Paris, France, Working Papers 2018/03, 2018, doi: 10.1787/dd98ff58-en.
[2] V. Hunt, *Smart Robots: A Handbook of Intelligent Robotic Systems* (Chapman & Hall Advanced Industrial Technology Series). New York, NY, USA: Chapman & Hall, 1985, doi: 10.1007/978-1-4613-2533-8.
[3] S. Zeghloul, M. A. Laribi, and J.-P. Gazeau, *Robotics and Mechatronics*. Cham, Switzerland: Springer, 2015, doi: 10.1007/978-3-319-22368-1.
[4] A. Codourey, "Dynamic modeling of parallel robots for computed-torque control implementation," *Int. J. Robot. Res.*, vol. 17, no. 12, pp. 1325–1336, Dec. 1998.
[5] J.-J. E. Slotine and W. Li, "On the adaptive control of robot manipulators," *Int. J. Robot. Res.*, vol. 6, no. 3, pp. 49–59, 1987.
[6] G. Tao, *Adaptive Control Design and Analysis*, vol. 37. Hoboken, NJ, USA: Wiley, 2003.
[7] K. D. Young and Ü. Özgüner, *Variable Structure Systems, Sliding Mode and Nonlinear Control*, vol. 247. London, U.K.: Springer, 1999, doi: 10.1007/BFb0109967.
[8] C. Edwards, E. F. Colet, L. Fridman, E. F. Colet, and L. M. Fridman, *Advances in Variable Structure and Sliding Mode Control*, vol. 334. Berlin, Germany: Springer, 2006, doi: 10.1007/11612735.
[9] I. Cervantes and J. Alvarez-Ramirez, "On the PID tracking control of robot manipulators," *Syst. Control Lett.*, vol. 42, no. 1, pp. 37–46, Jan. 2001.
[10] Y. Su, P. C. Müller, and C. Zheng, "Global asymptotic saturated PID control for robot manipulators," *IEEE Trans. Control Syst. Technol.*, vol. 18, no. 6, pp. 1280–1288, Nov. 2010.
[11] F. L. Lewis, D. Vrabie, and V. L. Syrmos, *Optimal Control*. Hoboken, NJ, USA: Wiley, 2012.
[12] G. Zong, H. Ren, and H. R. Karimi, "Event-triggered communication and annular finite-time $H\infty$ filtering for networked switched systems," *IEEE Trans. Cybern.*, vol. 51, no. 1, pp. 309–317, Jan. 2021.
[13] G. Zong, W. Qi, and H. R. Karimi, "L_1 control of positive semi-Markov jump systems with state delay," *IEEE Trans. Syst., Man, Cybern. Syst.*, early access, Mar. 24, 2020, doi: 10.1109/TSMC.2020.2980034.
[14] G. Zong, Y. Li, and H. Sun, "Composite anti-disturbance resilient control for Markovian jump nonlinear systems with general uncertain transition rate," *Sci. China Inf. Sci.*, vol. 62, no. 2, p. 22205, Feb. 2019.
[15] G. Bartolini, L. Fridman, A. Pisano, and E. Usai, *Modern Sliding Mode Control Theory: New Perspectives and Applications*, vol. 375. Berlin, Germany: Springer, 2008, doi: 10.1007/978-3-540-79016-7.
[16] J. Y. Hung, W. Gao, and J. C. Hung, "Variable structure control: A survey," *IEEE Trans. Ind. Electron.*, vol. 40, no. 1, pp. 2–22, Feb. 1993.
[17] A. Levant, "Chattering analysis," *IEEE Trans. Autom. Control*, vol. 55, no. 6, pp. 1380–1389, Jun. 2010.

[18] V. I. Utkin and H. Lee, "The chattering analysis," in *Proc. 12th Int. Power Electron. Motion Control Conf.*, Aug. 2006, pp. 2014–2019.
[19] C. Mu and H. He, "Dynamic behavior of terminal sliding mode control," *IEEE Trans. Ind. Electron.*, vol. 65, no. 4, pp. 3480–3490, Apr. 2018.
[20] C. U. Solis, J. B. Clempner, and A. S. Poznyak, "Fast terminal sliding-mode control with an integral filter applied to a van der pol oscillator," *IEEE Trans. Ind. Electron.*, vol. 64, no. 7, pp. 5622–5628, Jul. 2017.
[21] S. S.-D. Xu, C.-C. Chen, and Z.-L. Wu, "Study of nonsingular fast terminal sliding-mode fault-tolerant control," *IEEE Trans. Ind. Electron.*, vol. 62, no. 6, pp. 3906–3913, Jun. 2015.
[22] A. T. Vo and H.-J. Kang, "An adaptive neural non-singular fast-terminal sliding-mode control for industrial robotic manipulators," *Appl. Sci.*, vol. 8, no. 12, p. 2562, Dec. 2018.
[23] A. T. Vo and H.-J. Kang, "An adaptive terminal sliding mode control for robot manipulators with non-singular terminal sliding surface variables," *IEEE Access*, vol. 7, pp. 8701–8712, 2019.
[24] A. T. Vo, H.-J. Kang, and T. N. Truong, "A fast terminal sliding mode control strategy for trajectory tracking control of robotic manipulators," in *Proc. Int. Conf. Intell. Comput.*, 2020, pp. 177–189.
[25] H. Lee, E. Kim, H.-J. Kang, and M. Park, "A new sliding-mode control with fuzzy boundary layer," *Fuzzy Sets Syst.*, vol. 120, no. 1, pp. 135–143, May 2001.
[26] A. T. Vo and H.-J. Kang, "A novel fault-tolerant control method for robot manipulators based on non-singular fast terminal sliding mode control and disturbance observer," *IEEE Access*, vol. 8, pp. 109388–109400, 2020.
[27] T. N. Truong, H.-J. Kang, and A. T. Vo, "An active disturbance rejection control method for robot manipulators," in *Proc. Int. Conf. Intell. Comput.*, 2020, pp. 190–201.
[28] T. N. Truong, A. T. Vo, and H.-J. Kang, "Implementation of an adaptive neural terminal sliding mode for tracking control of magnetic levitation systems," *IEEE Access*, vol. 8, pp. 206931–206941, 2020.
[29] T. N. Truong, H.-J. Kang, and T. D. Le, "Adaptive neural sliding mode control for 3-DOF planar parallel manipulators," in *Proc. 3rd Int. Symp. Comput. Sci. Intell. Control*, Sep. 2019, pp. 1–6.
[30] K. Shyam, C. Asif, J. A. Moreno, L. Fridman, and B. Bandopadhyay, "Higher order super-twisting algorithm," in *Proc. 13th Int. Workshop Variable Struct. Syst. (VSS)*. Nantes, France: IEEE Press, Jun./Jul. 2014, doi: 10.1109/VSS.2014.6881129.
[31] B. Yoo and W. Ham, "Adaptive fuzzy sliding mode control of nonlinear system," *IEEE Trans. Fuzzy Syst.*, vol. 6, no. 2, pp. 315–321, May 1998.
[32] K. Mei and S. Ding, "Second-order sliding mode controller design subject to an upper-triangular structure," *IEEE Trans. Syst., Man, Cybern. Syst.*, vol. 51, no. 1, pp. 497–507, Jan. 2021.
[33] J. Yuan, S. Ding, and K. Mei, "Fixed-time SOSM controller design with output constraint," *Nonlinear Dyn.*, vol. 102, no. 3, pp. 1567–1583, Nov. 2020.
[34] A. T. Vo and H.-J. Kang, "Adaptive neural integral full-order terminal sliding mode control for an uncertain nonlinear system," *IEEE Access*, vol. 7, pp. 42238–42246, 2019.
[35] M. Rubagotti, A. Estrada, F. Castanos, A. Ferrara, and L. Fridman, "Integral sliding mode control for nonlinear systems with matched and unmatched perturbations," *IEEE Trans. Autom. Control*, vol. 56, no. 11, pp. 2699–2704, Nov. 2011.
[36] V. Utkin and J. Shi, "Integral sliding mode in systems operating under uncertainty conditions," in *Proc. 35th IEEE Conf. Decis. Control*, vol. 4, Dec. 1996, pp. 4591–4596.
[37] S. Laghrouche, F. Plestan, and A. Glumineau, "Higher order sliding mode control based on integral sliding mode," *Automatica*, vol. 43, no. 3, pp. 531–537, Mar. 2007.
[38] A. T. Vo and H.-J. Kang, "A chattering-free, adaptive, robust tracking control scheme for nonlinear systems with uncertain dynamics," *IEEE Access*, vol. 7, pp. 10457–10466, 2019.
[39] C.-S. Chiu, "Derivative and integral terminal sliding mode control for a class of MIMO nonlinear systems," *Automatica*, vol. 48, no. 2, pp. 316–326, Feb. 2012.
[40] L. Qiao and W. Zhang, "Adaptive non-singular integral terminal sliding mode tracking control for autonomous underwater vehicles," *IET Control Theory Appl.*, vol. 11, no. 8, pp. 1293–1306, May 2017.
[41] A. T. Vo, H.-J. Kang, and T. D. Le, "An adaptive fuzzy terminal sliding mode control methodology for uncertain nonlinear second-order systems," in *Proc. Int. Conf. Intell. Comput.*, 2018, pp. 123–135.
[42] A. T. Vo, H.-J. Kang, and T. D. Le, "Full-order sliding mode control algorithm for robot manipulators using an adaptive radial basis function neural network," in *Proc. Int. Conf. Intell. Comput.*, 2019, pp. 155–166.
[43] M. Van, X. P. Do, and M. Mavrovouniotis, "Self-tuning fuzzy PID-nonsingular fast terminal sliding mode control for robust fault tolerant control of robot manipulators," *ISA Trans.*, vol. 96, pp. 60–68, Jan. 2020.
[44] T. Salloom, X. Yu, W. He, and O. Kaynak, "Adaptive neural network control of underwater robotic manipulators tuned by a genetic algorithm," *J. Intell. Robot. Syst.*, vol. 97, nos. 3–4, pp. 657–672, Mar. 2020.
[45] L. Wu, Q. Yan, and J. Cai, "Neural network-based adaptive learning control for robot manipulators with arbitrary initial errors," *IEEE Access*, vol. 7, pp. 180194–180204, 2019.
[46] J. J. Craig, *Introduction to Robotics: Mechanics and Control*. London, U.K.: Pearson Education India, 2009.
[47] M. Van and D. Ceglarek, "Robust fault tolerant control of robot manipulators with global fixed-time convergence," *J. Franklin Inst.*, vol. 358, no. 1, pp. 699–722, Jan. 2021.
[48] B. Jiang, M. Staroswiecki, and V. Cocquempot, "Fault accommodation for nonlinear dynamic systems," *IEEE Trans. Autom. Control*, vol. 51, no. 9, pp. 1578–1583, Sep. 2006.
[49] Q. V. Doan, A. T. Vo, T. D. Le, H.-J. Kang, and N. H. A. Nguyen, "A novel fast terminal sliding mode tracking control methodology for robot manipulators," *Appl. Sci.*, vol. 10, no. 9, p. 3010, Apr. 2020.
[50] Y. Shtessel, C. Edwards, L. Fridman, and A. Levant, *Sliding Mode Control and Observation*. New York, NY, USA: Springer, 2014, doi: 10.1007/978-0-8176-4893-0.
[51] H. Pan, G. Zhang, H. Ouyang, and L. Mei, "Novel fixed-time non-singular fast terminal sliding mode control for second-order uncertain systems based on adaptive disturbance observer," *IEEE Access*, vol. 8, pp. 126615–126627, 2020.
[52] V. I. Utkin and A. S. Poznyak, "Adaptive sliding mode control," in *Advances in Sliding Mode Control*. Berlin, Germany: Springer, 2013, pp. 21–53.

THANH NGUYEN TRUONG received the Engineering degree in electrical engineering from the University of Science and Technology, Danang, Vietnam, in 2018. He is currently pursuing the Ph.D. degree with the Department of Electrical Engineering, University of Ulsan, Ulsan, South Korea. His major studying activities involve machine learning, sliding mode control, and robotic manipulators.

ANH TUAN VO received the B.S. degree in electrical engineering from the Danang University of Technology, Danang, Vietnam, in 2008, the M.S. degree in automation from The University of Danang—Danang University of Science and Technology, Danang, in 2013, and the Ph.D. degree in electrical engineering from The Graduate School of the University of Ulsan, Ulsan, South Korea, in 2021. He has published more than 20 papers in journals and international conferences. His research interests include intelligent control, sliding mode control and its applications, and fault-tolerant control.

HEE-JUN KANG received the B.S. degree in mechanical engineering from Seoul National University, South Korea, in 1985, and the M.S. and Ph.D. degrees in mechanical engineering from The University of Texas at Austin, USA, in 1988 and 1991, respectively. Since 1992, he has been a Professor of electrical engineering with the University of Ulsan. His current research interests include sensor-based robotic applications, robot calibration, haptics, robot fault diagnosis, and mechanism analysis.